Multimaterial Topology Optimization of Electric Machines Based on Normalized Gaussian Network

Takahiro Sato[1,3], Kota Watanabe[2], and Hajime Igarashi[1], *Member, IEEE*

[1] Graduate school of Information science and technology, Hokkaido University,
Kita 14, Nishi 9, Kita-ku, Sapporo, 060-0814, JAPAN, [2] Muroran Institute of Technology, [3] JSPS Research Fellow

This paper presents a topology optimization method for multimaterial models based on the normalized Gaussian network (NGnet). In this method, one can determine optimal shapes of machines which are composed of various materials such as iron, magnet and non-magnetic material. The present method is applied to the optimization of interior permanent magnet motor to determine the distributions of magnetic core and flux barrier as well as magnets. The optimization results show that average torque can be improved using as small amount of magnet as possible. In addition, characteristic of the present method is discussed in detail.

***Index Terms*—interior permanent magnet motor, topology optimization.**

I. Introduction

Topology optimization allows us to find novel shapes of electric machines and devices. For example, the rotor shape of interior permanent magnet (IPM) motor has been optimized with little dependence on experience and knowledge of engineers [1]-[3]. One of the well-known topology optimization methods is the on/off method with evolutionary algorithms (EA) [1],[2],[5], in which the optimization model is subdivided into small cells to which binary states, on (material) and off (air), are assigned. The model shape is optimized for the binary states using EA. Although the on/off method with EA possibly finds good approximations to global optimal solutions without sensitivity analysis unlike the level-set methods [3],[4], we often obtain quite complicated shapes which are not suitable for manufacturing. The spatial filtering has been applied to the optimization processes to reduce spatial frequency in the shapes [2],[5]. However, because the resultant shapes strongly depend on the employed filtering and its parameters, we must carefully tune them to obtain desirable solutions.

To obtain smooth shapes without filtering, the authors have introduced the topology optimization method based on Normalized Gaussian Network (NGnet) [6]. Although this method can easily find smooth optimal shapes, multiple material distributions cannot be considered. In this paper, we present the NGnet-based multimaterial topology optimization method (NGnet-MTO), which can determine the optimal distribution of various materials such as iron, magnet, and non-magnetic material. Moreover, NGnet-MTO can globally seek for heuristic optima using the Genetic Algorithm with the heuristic local search.

The NGnet-MTO is applied to the optimization of rotor shape in an IPM motor in which distributions of magnetic core and flux barrier as well as magnets are determined. It will be shown that smooth rotor shapes can be obtained and the average torque of an IPM motor can be improved using as small amount of magnet as possible. In addition, the characteristic of the present method will be discussed in detail.

Manuscript received May 23, 2014. Corresponding author: Takahiro Sato (e-mail: tsato@em-si.eng.hokudai.ac.jp).
Digital Object Identifier inserted by IEEE

II. Multimaterial Optimization using NGnet

A. NGnet-based topology optimization method

In NGnet-MTO, the device shapes are determined based on the output of NGnet which is computed from the weighted sum of normalized Gaussians [7], as shown in Fig. 1. Because of this definition, the NGnet-output is spatially smooth. The output of NGnet, $f(\boldsymbol{x})$, is given by

$$f(\boldsymbol{x}) = \sum_{i=1}^{N} w_i b_i(\boldsymbol{x}), \tag{1}$$

$$b_i(\boldsymbol{x}) = G_i(\boldsymbol{x}) \Big/ \sum_{k=1}^{N} G_k(\boldsymbol{x}), \tag{2}$$

where $\boldsymbol{x}$ is position vector, N is the number of Gaussians, and $G_k(\boldsymbol{x})$ is the Gaussian function. Moreover, w_i is the weight for $b_i(\boldsymbol{x})$. The state of the cell e in the design region is determined from $f(\boldsymbol{x})$. For example, when we consider the binary state {on, off} for each cell, the cell state is determined as follows: when $f(\boldsymbol{x}_e) \geq 0 (< 0)$, $S_e \leftarrow on(off)$, where $\boldsymbol{x}_e$ is the center of e. When considering multiple states, S_e can be determined through the combination of outputs of NGnets. For example, four material states can be expressed using two NGnets. For simplicity, in this work, we uniformly deploy the Gaussians to cover design region, and all the Gaussian have the same isotropic deviations.

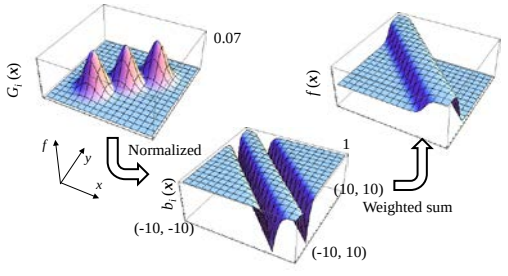

Fig. 1. Output of NGnet in case of 2D input.

B. Optimization algorithm

In NGnet-MTO, we consider the chromosome $\boldsymbol{w}=\{w_1, w_2, \ldots w_{N\times NG}\}$ for the real-coded Genetic Algorithm (GA), named

AREX+JGG [8], where N_G denotes the number of NGnets. Each entity w_i of $\boldsymbol{w}$ is rounded to -1/+1 in order to reduce search space. Figure 2 demonstrates the representation of four-material model generated from $\boldsymbol{w}$ where N=9 and N_G=2. Once $\boldsymbol{w}$ is determined, then the outputs of two NGnets, $f_1(\boldsymbol{x}_e)$ and $f_2(\boldsymbol{x}_e)$, in cell e are computed from (1). The state of each cell is determined from $f_1(\boldsymbol{x}_e)$ and $f_2(\boldsymbol{x}_e)$, as shown in Fig. 2.

To cover the design region by Gaussians, enough number of Gaussians must be placed, which results in long chromosome size. This leads to long computational time which is necessary for search in high dimensional space. In addition, the fitness of individuals is computed in parallel [1]. Moreover, the heuristic local search (LS) is employed, because original GA hardly finds even heuristic local optima when chromosome size is long. For LS, the modified greedy method is employed and applied to the elite individual. In this method, one randomly-selected gene is inverted (e.g. +1→-1). If the fitness after the inversion is better than before, the inverted gene is adopted. Then, other gene is again randomly selected and inverted. This process is repeated until all genes are selected. Namely, the genes are greedily changed to improve fitness. Note that the resultant chromosome after this procedure depends on the order of the selection. Hence, the parallel computation technique is also employed for LS, that is, we set different selection orders, and the greedy search is applied to them in parallel. The flow of the optimization algorithm is shown in Fig. 3.

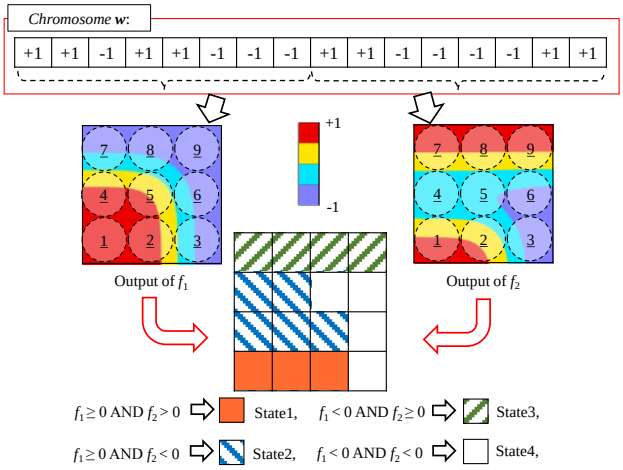

Fig. 2. Representation of multimaterial distributions using NGnets.

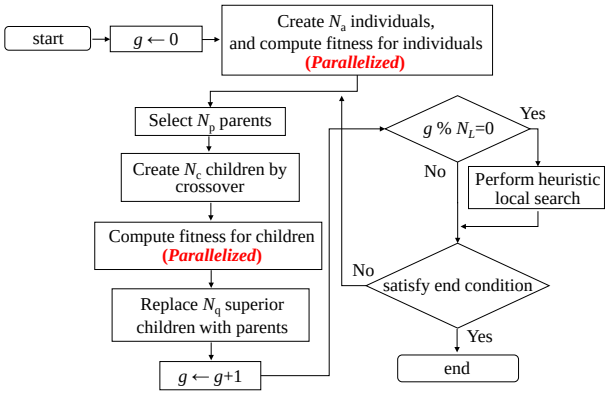

Fig. 3. Flow of parallelized NGnet-MTO.

III. Optimization of IPM Motor

A. Problem setting

The rotor shape of the IEEJ D-model (initial model) [9] shown in Fig. 4, which is a benchmark model for testing numerical methods, is optimized using NGnet-MTO. The purpose of the optimization is to maximize the average torque using as small amount of magnet as possible. The torque is analyzed by the finite element method (FEM), where the motor is driven by three-phase sinusoidal current whose amplitude I and phase angle β are $3A_{rms}$ and 20deg respectively, and the nonlinear BH curve of 50H350 is assumed. Figure 5 shows the design region which contains 3870 FEs. The rotor shape in the domain next to the design region is created assuming right-left symmetry. The distribution of magnets, magnetic core, and flux barrier in the design region is optimized. The optimization problem is formulated by

$$F = -T_{ave}/T_0 \rightarrow \min., \tag{3}$$

$$\text{sub. to} \quad S \leq KS_T, \quad S_D < 0.05S, \quad R_{\max} < R_{th}, \quad \rho_{\max} < \rho_{th}, \tag{4}$$

where T_{ave} and S denote average torque and magnet area, respectively, S_D is critical area below which the magnet is degaussed when I and β are $4.5A_{rms}$ and 90deg, respectively. In addition, T_0=2.2Nm and S_T=52.5mm^2 are the torque and magnet area of the initial model, respectively, and K is a weighting coefficient. Moreover, R_{th}=27.8mm, ρ_{th}=324MPa

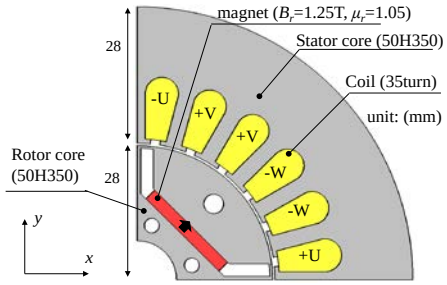

Fig. 4. IEEJ D-model (initial model) [9].

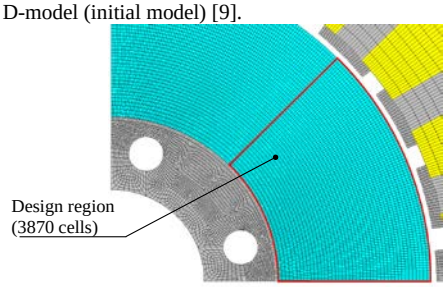

Fig. 5. Cells in design region.

are mechanical thresholds, and $R_{\max}$, $\rho_{\max}$ are the maximum displacement and stress in the rotor, respectively, when the motor angular velocity is 2500rpm, where they are computed by the mechanical FEM.

To treat four constraints efficiently, we employ the oracle penalty method [10] in which penalty is dynamically controlled. This method allows us to avoid the situation that the penalty becomes overwhelmingly dominant in F.

B. Optimization setting

In this work, we consider two magnets which have different directions in magnetization, that is, *mag*1 and *mag*2 whose magnetization vectors, $\boldsymbol{M}/\|\boldsymbol{M}\|$, are (0, 1) and $(1/\sqrt{2}, 1/\sqrt{2})$, respectively. The state S_e for an element e is determined based on output of two NGnets, $f_1(\boldsymbol{x})$ and $f_2(\boldsymbol{x})$, as follows:

$$S_e \leftarrow \begin{cases} mag1 & f_1(\boldsymbol{x}_e) \geq 0 \text{ AND } f_2(\boldsymbol{x}_e) \geq 0, \\ mag2 & f_1(\boldsymbol{x}_e) < 0 \text{ AND } f_2(\boldsymbol{x}_e) \geq 0, \\ \text{core} & f_1(\boldsymbol{x}_e) \geq 0 \text{ AND } f_2(\boldsymbol{x}_e) < 0, \\ \text{air} & f_1(\boldsymbol{x}_e) < 0 \text{ AND } f_2(\boldsymbol{x}_e) < 0. \end{cases} \quad (5)$$

The parameters in NGnet-MTO are summarized in Table I, and the optimization is performed over 60 generations. In this setting, it takes about 5 days to obtain final solution using the *Intel Xeon CPU* (2.1GHz, 12 cores).

TABLE I
PARAMETER SETTING IN NGNET-MTO

Initial individuals:N_a	Num .of parents:N_p	Num. of replaced parents:N_q	Num. of children: N_c	Interval between LS: N_L
800	120	40	100	20

C. Optimization Results

It is expected that the resultant solution obtained by NGnet-MTO depends on the number of deployed Gaussians and the deviation. To clarify its effect on optimization results, we test for three different distributions shown in Fig. 6. Larger number of Gaussians increases shape representation ability, and simultaneously, the chromosome size gets long. In (C), the chromosome size is equal to that of (B), while the diameter of Gaussians is set quite small. In this case, S_e is determined from the output of the nearest Gaussian, that is, it works like the cluster filtering [2]. The optimization is performed five times for each distribution in which K in (4) is set to 1.

Figure 7 shows the changes in average fitness during optimizations with and without LS. We can see that the average fitness in (A) and (B) are almost identical when using LS, while the average fitness in (A) is worse than that in (B) without LS. These results show that LS accelerates progress in the optimization.

The changes in average fitness for three cases with LS are shown in Fig. 8, from which it can be seen that the fitness in (C) is worse than those in (A) and (B). This result is attributed to the fact that the representation ability in (C) is lower than the others. Figure 9 shows the resultant shapes of the best solution for three distributions. All solutions have smooth and connected material regions which would be suitable for engineering realization. We can find that all the results have V-shaped magnets. Moreover, the average torques in (A) and (B) are larger than that in the initial model, although the magnet volume is not increased. From Fig. 9(c), we can see that rectangle-shaped magnets are obtained in (C). Although such shapes are quite suitable for manufacturing, there is little torque improvement. When the diameter of Gaussian is small, the representation ability is strongly limited because S_e is determined only by the nearest output. This is the reason why

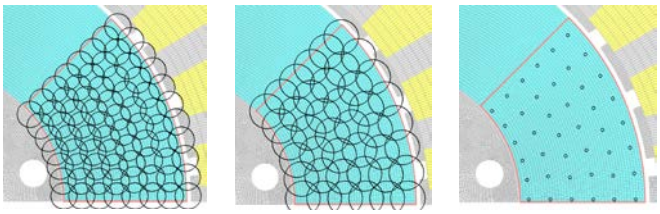

(A): 76 Gaussians (B): 42 Gaussians (C): 42 Gaussians with small diameter

Fig. 6. Deployed Gaussians used in optimization.

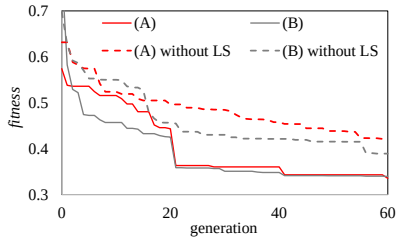

Fig. 7. Changes in average fitness with and without local search.

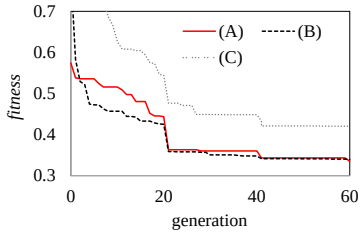

Fig. 8. Changes in average fitness during optimization process.

the average fitness is worst in the three cases.

The torque waves for the optimized shapes are shown in Fig. 10. Because torque ripple is not considered in the objective, the ripple is not sufficiently improved. However, the resultant rotor in (A) has lower torque ripple compared with those of the initial model. It has been pointed out in [11] that V-shaped magnets cause the torque reduction when the permeability distribution is asymptotic. In this problem, armature current is not so strong that permeability distribution is nearly symmetric as shown in Fig. 11. This would be the reason why V-shaped magnets are obtained by which the average torques are improved.

A multi-start algorithm based on LS without GA would also be effective for NGnet-MTO. Thus, this approach is tested for the distribution (A), in which 30 individuals are randomly generated and LS is applied to them for three times. The performance of the best solution obtained by the multi-start algorithm is summarized in Table II which also contains the performance for Fig. 9(a), for comparison. It is clear that the solution obtained by the multi-start LS is inferior to that shown in Fig. 9(a). This fact suggests the superiority of the LS combined with GA. This is because fitness-landscape in this problems is complex and multimodal due to four constraints. In such condition, it is difficult to find good heuristic solutions only by LS.

The optimization is performed by setting K=0.6. The resultant shape using (B) is shown in Fig. 12(a) in which we can see that the optimized shape is again smooth and its torque reduction is about 15% while magnet volume is 60%. From this result, the effectiveness in NGnet-MTO is shown under the different constraint condition.

(a): resultant shape for (A) (T_{ave}=1.17T_0, S=0.99S_T, S_D=0.07%)
(b): resultant shape for (B) (T_{ave}=1.16T_0, S=0.97S_T, S_D=0.86%)
(c): resultant shape for (C) (T_{ave}=1.01T_0, S=0.97S_T, S_D=0.2%)

Fig. 9. Resultant rotor shapes for three Gaussian distributions, where light and deep red areas correspond to *mag*1 and *mag*2, respectively.

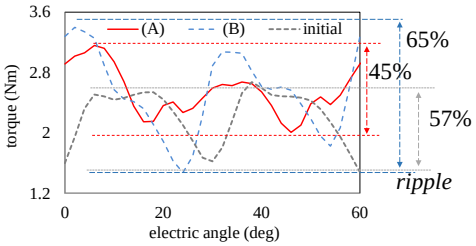

Fig. 10. Torque waves for resultant solutions

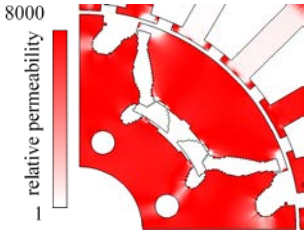

Fig. 11. Permeability distribution in rotor core for (A).

TABLE II
BEST SOLUTION OBTAINED BY MULTI-START LS

	fitness	T_{ave}	S	S_D
GA+LS (Fig. 9(a))	0.26	1.17T_0	0.99S_T	0.07%
multi-start LS	0.48	0.90T_0	0.93S_T	1.3%

Moreover, the optimization result is compared with that obtained by the conventional on/off method with clustering and cleaning filtering [2], [5]. In the filtering, the material islands composed of smaller than three elements are eliminated. The other settings are the same as the previous optimizations. Figure 12(b) shows the resultant shape obtained by the conventional method. Because of huge number of target FEs, the filtering does not effectively work, and complicated shape is obtained. This result suggests that, in the conventional method, the filtering parameter must carefully be tuned to obtain smooth shapes with desirable performance.

From these results, we can conclude that NGnet-MTO with LS can lead to smooth optimized shapes whose performance is satisfactory. The LS is effective when combined with GA, especially for the model which contains large number of Gaussians. The small diameter of Gaussians leads to simple structures, while the shape representation ability is limited and it highly depends on the deployed Gaussians.

IV. CONCLUSIONS

The NGnet-MTO has been introduced. It has been applied to shape optimization of an IPM motor. It has been shown that NGnet-MTO can find smooth shapes which have improved

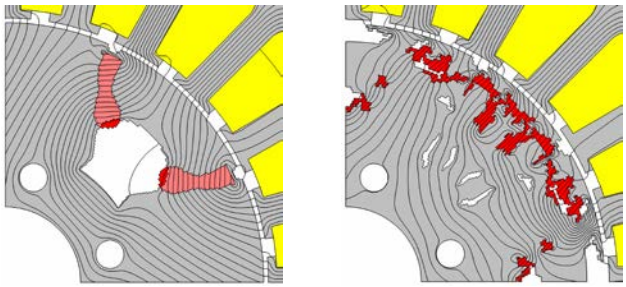

(a): when K=0.6 (T_{ave}=0.86T_0, S=0.59S_T, S_D=0.4%)
(b): conventional method (T_{ave}=0.64T_0, S=0.83S_T, S_D=0.47%)

Fig. 12. Resultant rotor shapes obtained by different settings.

torques. The heuristic local search is effective for the progress acceleration, especially for models which have many Gaussians.

REFERENCES

[1] Y. Okamoto, Y. Tominaga, S. Wakao, S. Sato, "Topology Optimization of Rotor Core Combined With Identification of Current Phase Angle in IPM Motor Using Multistep Genetic Algorithm," *IEEE Trans. Magn.*, vol. 50, no. 2, 2014, 7017904.

[2] T. Ishikawa, K. Nakayama, N. Kurita, F. P. Dawson, "Optimization of Rotor Topology in PM Synchronous Motors by Genetic Algorithm Considering Cluster of Materials and Cleaning Procedure," *IEEE Trans. Mang.*, vol. 50, no. 2, 2014, 7015704.

[3] P. Putek, P. Paplicki, R. Palka, "Low Cogging Torque Design of Permanent Magnet Machine Using Modified Multi-Level Set Method With Total Variation Regularization," *IEEE Trans. Magn.*, vol. 50, no. 2, 2014, 7016204.

[4] J. Lee, S. Wang, "Topological Shape Optimization of Permanent Magnet in Voice Coil Motor Using Level Set Method," *IEEE Trans. Magn.*, vol. 48, no. 2 pp. 931-934, 2012.

[5] T. Sato, K. Watanabe, H. Igarashi, "A Modified Immune Algorithm with Spatial Filtering for Multiobjective Topology Optimization of Electromagnetic device," *COMPEL*, vol. 33, no. 3, pp.821-833, 2014.

[6] T. Sato, K. Watanabe, H. Igarashi, "A Topology Optimization method for Electric Machines Based on Normalized Gaussian Network," *IEEJ Joint Tech. Meeting on Static Apparatus and Rotating Machinery*, pp. 17-22, 2013. (in Japanese)

[7] J. Moody, "Fast Learning in Networks of Locally-Tuned Processing Units," *Neural Computation*, vol. 1, No. 2, pp. 281-294, 1989.

[8] A. Komori, *et .al.*, "Efficient Numerical Optimization Algorithm Based on New Real-Coded Genetic Algorithm, AREX+JGG, and Application to the Inverse Problem in Systems Biology," *Applied Mathematics*, vol. 3, no. 10, pp. 1463-1470, 2012.

[9] IEEJ Investigating R&D committee, "IEEJ Technical Report," *Inst. Electr. Eng. Japan, Tech. Rep*. No. 776, 2000. (in Japanese)

[10] M. Schlüter, M. Gerdts, "The oracle penalty method," *J. Glob. Optim.*, vol. 47, no. 2, pp. 293-325, 2010.

[11] K. Yamazaki, M. Kumagai, "Rotor Design of Interior Permanent Magnet Motors Considering Cross Magnetization Caused by Magnetic Saturation," *IEEE Trans. Ind. Appl.*, vol. 57, no. 1, pp. 61-69, 2010.